



Faculty Scholarship

2016

On gigahertz spectral turnovers in pulsars

K. Rajwade

D. R. Lorimer

L. D. Anderson

Follow this and additional works at: https://researchrepository.wvu.edu/faculty_publications

Digital Commons Citation

Rajwade, K.; Lorimer, D. R.; and Anderson, L. D., "On gigahertz spectral turnovers in pulsars" (2016). *Faculty Scholarship*. 257.
https://researchrepository.wvu.edu/faculty_publications/257

This Article is brought to you for free and open access by The Research Repository @ WVU. It has been accepted for inclusion in Faculty Scholarship by an authorized administrator of The Research Repository @ WVU. For more information, please contact ian.harmon@mail.wvu.edu.

On gigahertz spectral turnovers in pulsars

K. Rajwade*, D. R. Lorimer, L. D. Anderson

Department of Physics and Astronomy, West Virginia University, Morgantown, WV 26506, USA

28 July 2018

ABSTRACT

Pulsars are known to emit non-thermal radio emission that is generally a power-law function of frequency. In some cases, a turnover is seen at frequencies around 100 MHz. Kijak et al. have reported the presence of a new class of “Gigahertz Peaked Spectrum” (GPS) pulsars that show spectral turnovers at frequencies around 1 GHz. We apply a model based on free-free thermal absorption to explain these turnovers in terms of surrounding material such as the dense environments found in H II regions, Pulsar Wind Nebulae (PWNe), or in cold, partially ionized molecular clouds. We show that the turnover frequency depends on the electron temperature of the environment close to the pulsar, as well as the emission measure along the line of sight. We fitted this model to the radio fluxes of known GPS pulsars and show that it can replicate the GHz turnover. From the thermal absorption model, we demonstrate that normal pulsars would exhibit a GPS-like behaviour if they were in a dense environment. We discuss the application of this model in the context of determining the population of neutron stars within the central parsec of the Galaxy. We show that a non-negligible fraction of this population might exhibit high-frequency spectral turnovers, which has implications on the detectability of these sources in the Galactic centre.

Key words: stars: neutron — pulsars: general — Galaxy:centre

1 INTRODUCTION

Radio flux measurements from pulsars have revealed a wealth of information about the underlying physical processes involved in coherent radio emission (for a review, see Graham-Smith 2003). A knowledge of the spectral behaviour of pulsars is also important for population studies that seek to constrain the luminosity function of the underlying population (e.g., Bates et al. 2014). Studies in the past have shown that the flux density, S , as a function of frequency, ν , for a pulsar can be described by a simple power law $S \propto \nu^\alpha$, with a spectral index α (e.g., Lorimer et al. 1995). Although the observed spectra are found to have a mean value of α around -1.6 (Maron et al. 2000), population models suggest that the underlying population is more consistent with a normal distribution of spectral indices with the mean value around -1.4 (Bates et al. 2013). A small fraction of such sources ($\sim 10\%$) show a broken power-law behaviour, with α of ~ -0.9 and ~ -2.2 (Maron et al. 2000). At low frequencies, synchrotron self absorption becomes dominant in the pulsar magnetosphere and the spectrum tends to show a turnover (Sieber 1973). Such turnovers have been detected for many pulsars around ~ 100 MHz. An excellent example of such a spectrum can be found for PSR B0329+54 in Kramer et al. (2003).

In 2007, a new class of pulsars was proposed. As described by Kijak et al. (2007, 2011; hereafter K07 and K11), these “Gigahertz Peaked Spectrum” (GPS) pulsars show a spectral turnover at frequencies ~ 1 GHz. To date, eleven GPS pulsars have been reported of which two are magnetars (K07, K11, Dembska et al. 2014, Lewandowski et al 2015). These authors have found a correlation between the spectral shape of pulsars showing such behaviour and the environment around the pulsar. The strongest argument for environmental origins of high-frequency turnover came from the observations of the binary pulsar B1259–63 (Kijak et al. 2011; hereafter K11a). This pulsar exhibits GPS-like behaviour when it is close to its companion Be star LS 2883 and shows a single power-law spectrum when it is far from the Be star. In another study, Kijak et al. (2013) obtained spectra for two magnetars that show GPS-like behaviour. Both of the magnetars are associated with supernova remnants (SNRs). The presence of these dense, ionized regions around the pulsars suggests that free-free absorption by the surrounding ionized gas could be responsible for high-frequency turnovers. The authors concluded that pulsars located within ionized environments such as SNRs, H II regions, and PWNe that have high electron densities and emission measures should invariably have high-frequency spectral turnovers.

Motivated by these ideas, a very recent study by Lewandowski et al. (2015) applied a similar model to the

*Email: kmrajwade@mix.wvu.edu

one presented here. They show that the absorption is dominant in moderately cold plasma ($T_e \sim 5000 - 8000$ K) with heightened electron densities (above $\sim 1000 \text{ cm}^{-3}$ pc). They use their model to show that the rapid variations in the spectrum of radio magnetar SGR 1745–2900 in the Galactic centre can be explained by free-free thermal absorption of the radio emission by ejecta surrounding the magnetar. Using simulations, they were able to show that pulsars can exhibit GPS behaviour that can be explained by the model. This is compelling evidence of the dependence of pulsar spectra on their surroundings.

Thermal absorption by free electrons in the vicinity of the GPS pulsars may explain their spectral turnovers as proposed by Kijak et al (2011) and later by Kijak et al (2013). Radio emission from pulsars is known to have a steep spectrum that is believed to be due to a non-thermal emission process consisting of pair production in the magnetosphere (see, e.g., Contopoulos & Spitkovski 2006; Melrose et al. 2014). The characteristics of this emission are similar to those of radio emission observed from SNRs. In this paper, we modeled the emission from pulsars based on free-free absorption, which has previously been used to explain the radio emission from SNRs. A similar approach was taken by Lewandowski et al. (2015). In contrast to these authors, we have fitted this thermal absorption model to the six known GPS pulsars to constrain the Emission Measure (EM) along the line of sight based on known electron temperatures of the environment surrounding them. In addition, we consider multiple sources of absorbers and try to obtain the most suitable physical conditions for the observed spectrum. We also looked at one bright pulsar that does not show GPS behaviour. Using known parameters of EM and electron temperatures for PWNe, we simulated the spectrum of this source to that it can exhibit GPS behaviour and discuss about the pulsar’s low-frequency turnover. The model, procedure and results of our fitting are explained in section 2. In section 3, we discuss various implications of our results, and in particular highlight the importance of the model on the detectability of pulsars in the Galactic centre.

2 MODEL

2.1 Theory

Starting from the fundamental equation of radiative transfer (see, e.g., Burke & Smith 2014), we considered 2 scenarios: (i) the pulsar lies within the PWN/SNR or beyond an H II region; (ii) the pulsar lies beyond a cold, partially ionized molecular cloud. In either case, the total measured flux

$$S_{\text{obs},\nu} = S_{\text{psr},\nu} e^{-\tau_\nu} + S_{\text{reg},\nu} (1 - e^{-\tau_\nu}), \quad (1)$$

where $S_{\text{psr},\nu}$ is the pulsar’s intrinsic flux, $S_{\text{reg},\nu}$ is the flux of the intervening region (PWN or H II region) and τ_ν is the optical depth at frequency ν for this line of sight. We can ignore the $S_{\text{reg},\nu}$ term because it is a continuum emission that adds to the sky background. Assuming $\tau_\nu \sim \nu^{-2.1}$ for free-free absorption and assuming $\tau_\nu \ll 1$ for the frequencies of interest (Mezger & Henderson, 1967) we get

$$S_{\text{obs},\nu} = S_{\text{ref}} \left(\frac{\nu}{\nu_{\text{ref}}} \right)^\alpha \exp \left[-\tau_{\text{ref}} \left(\frac{\nu}{\nu_{\text{ref}}} \right)^{-2.1} \right]. \quad (2)$$

Here S_{ref} is some reference flux density measured at a reference frequency ν_{ref} , α is the spectral index and τ_{ref} is the optical depth at the reference frequency. This is similar to the model previously developed to fit spectra of SNRs (see, e.g., Dulk & Slee 1975).

To obtain the optical depth at a given frequency we used the expression given in Altenhoff et al. (1960) and Mezger & Henderson (1967) where we can assume that the medium is optically thin ($\tau \ll 1$) at high frequencies. Under this assumption, the optical depth

$$\tau = 0.082a \left(\frac{\nu}{\text{GHz}} \right)^{-2.1} \left(\frac{\text{EM}}{\text{cm}^{-6} \text{ pc}} \right) \left(\frac{T_e}{\text{K}} \right)^{-1.35}, \quad (3)$$

where a is a correction factor of the order unity for electron temperatures $T_e > 20$ K and EM is the emission measure. Using equations 2 and 3, we find the spectrum peaks at a frequency

$$\nu_{\text{peak}} = 0.433 \text{ GHz} (-\alpha)^{-0.476} \left(\frac{\text{EM}}{\text{cm}^{-6} \text{ pc}} \right)^{0.476} \left(\frac{T_e}{\text{K}} \right)^{-0.643}. \quad (4)$$

2.2 Application

We fitted equation 2 to the flux density spectra for six GPS pulsars reported in K11. The flux data were taken from K07, K11 and Dembska et al (2014). For PSR B1054–62 and PSR J1852–0635, the published errors on the fluxes (Dembska et al. 2014) were substantially smaller than the errors for other pulsars, which were around 20%. We therefore increased the errors on these two pulsars to make them comparable with the rest of the sample. We did this fitting for two scenarios: one for warm plasma with characteristic properties of H II regions or PWNe and one for cold, partially ionized clouds.

For the first scenario, we use characteristic properties of PWNe/H II regions, which are known to have $T_e \simeq 5000 - 10^4$ K for H II regions and $T_e \simeq 10^4 - 10^6$ K for PWNe (e.g., Slane et al. 2004). The value of T_e for the PWN/H II region scenario was fixed to 5000 K as Lewandowski et al. (2015) show that the absorption of radio emission takes place in plasma with ionized gas filaments with $T_e \sim 5000$ K in SNRs (Sankrit et al. 1998; Koo et al. 2007). Such high density plasma also exists in young “ultra compact” star forming H II regions where electron densities are of the order of $\sim 10^4 \text{ cm}^{-3}$ (for a review, see Churchwell 2002) so it is also possible that a pulsar lying beyond an H II region might experience absorption of radio emission. Pulsars within PWNe may not exhibit GPS spectra because the PWNe plasma distribution is inhomogeneous and there may not be a dense filament between us and the pulsar.

For the second scenario, we use characteristic properties of cold, partially ionized clouds, which Dulk & Slee 1975 suggest are the most promising absorbers of radio emission from SNRs. For such clouds, we used $T_e = 30$ K. Due to asymmetries in the PWN shell, the radio emission may be absorbed by the cold clouds instead of the filaments. However, PWN are often found in the vicinity of molecular clouds with a high rate of star formation. We kept α and τ as free parameters as we believe that there could be a bias in the measured values of α due to the high-frequency turnover behaviour. The value of EM can be calculated from the derived value of τ and by assuming a T_e . For this case, we assumed 30%

uncertainties in the value of T_e , and propagated this uncertainty to derive uncertainties in EM. The value of 30% is arbitrary in the sense that it only affects the errors on derived values of EM and not the values themselves. We select S_{ref} and the corresponding τ_{ref} from the highest frequency measurement since the effects of free-free absorption should be negligible at those frequencies and therefore the assumptions we made for τ_{ref} would hold. Using this as our starting point, we fitted the model to the observed spectra for the two different electron temperatures scenarios mentioned above using the Levenberg-Marquardt non-linear least squares algorithm (see, e.g., Press et al. 2010) and for each pulsar derived the values for EM and α given in Table 1.

The values of EM we derived in Table 1 have rarely been measured before. Here, we give a possible physical explanation of why such high values can arise. From the simulations done in Lewandowski et al. (2015), one infers that to observe GPS behaviour, a pulsar needs to be beyond a region of ionized gas a fraction of a parsec thick with ambient temperatures of the order of a few 1000 K and relatively high free electron density. High electron densities of ($\sim 2000 - 6000 \text{ cm}^{-3}$) with relatively cooler temperatures ($\sim 5000 - 8000 \text{ K}$) have been found to exist in dense filaments a fraction of a parsec wide around SNRs and PWNs (Sanskrit et al. 1998; Koo et al. 2007). For example, if we consider the line of sight along the filament found by Koo et al. in SNR G11.2-0.3, we can infer an EM contribution due to filament by using the values in their paper which is $\sim 10^7 \text{ cm}^{-6} \text{ pc}$. This is of the same order as our derived values. If we assume that the derived EM contributes to the total DM by a fraction a then the linear size of the filament

$$d_{\text{filament}} = a^2 \left(\frac{\text{DM}}{\text{cm}^{-3} \text{ pc}} \right)^2 \left(\frac{\text{EM}}{\text{cm}^{-6} \text{ pc}} \right) \text{ pc}. \quad (5)$$

The values obtained from Equation 5 reflect the dimension of the filament along the line of sight. For the absorbing medium, the mean electron density

$$\langle n_e \rangle = \frac{1}{a} \left(\frac{\text{DM}}{\text{cm}^{-3} \text{ pc}} \right)^{-1} \left(\frac{\text{EM}}{\text{cm}^{-6} \text{ pc}} \right) \text{ cm}^{-3}. \quad (6)$$

We estimate the electron density and the linear size of the absorber by assuming a DM fraction of 50% for the GPS sources in this paper. We did the analysis for the absorption scenarios considered for the previous analysis. From our results, we infer the most likely source of absorption for all the pulsars in our sample. The values of electron density, linear size and the source of absorption are listed in Table 2. The values we obtained for ν_{peak} differ from values given K11 simply because K11 calculate the turnover frequency from the intersection of two linear fits to the spectrum. To quantify the quality of the fit even further, we obtained the reduced χ^2 by fitting the pulsar fluxes with a single power law and compared them to the ones obtained by the model. The values for the power law are higher by at least a factor of two, suggesting that the model given in equation 2 is preferred over the power-law model.

The model fits the observed data well, as illustrated by Fig. 2 and the reduced χ^2 values given in Table 1. This motivated us to look at pulsars that do not lie in dense environments and to simulate their spectra to examine if the low-frequency turnover is due to the environment or

the pulsar itself. For this purpose, we selected one bright, non-GPS pulsar, PSR B0329+54, for which there are reliable estimates of flux densities at different frequencies and spectral index in literature (Kramer et al. 2003). Using the model, we tried to fit the spectrum of this pulsar. The slight turnover seen in the actual data for PSR B0329+54 is at $\sim 200 \text{ MHz}$. We believe that this turnover is intrinsic to the pulsar itself. Hence, the fit should give us values of EM due to ISM, or it may give some unreasonable values which might suggest a different mechanism for the low-frequency turnover seen in Fig. 1. To show this, we fitted for the EM of PSR B0329+54 by constraining the electron temperature, which we assume to be 5000 K (i.e., that of the Warm Ionized Medium (WIM) (Madsen et al. 2006)). The value we obtained was $5.2 \times 10^4 \text{ cm}^{-6} \text{ pc}$. If we assume a WIM-dominated ISM between the pulsar and the observer, we can use the measured parallax for PSR B0329+54 (Brisken et al. 2002) and its measured dispersion measure (DM), the integrated electron density along the line of sight to find a mean electron density of $\sim 0.024 \text{ cm}^{-3}$. Assuming a filling factor of 0.1 (Berkhuijsen and Muller 2008) to account for the clumpiness of the ISM, and knowing the distance to the pulsar, we derive a value of EM of $\sim 0.052 \text{ cm}^{-6} \text{ pc}$. This value of EM is ~ 6 orders of magnitude smaller than the one derived from the model which suggests that the turnover in spectrum of PSR B0329+54 could be due to synchrotron self-absorption in the pulsar's magnetosphere. Also, if we fix the EM to $\sim 0.052 \text{ cm}^{-6} \text{ pc}$ and fit for the electron temperature, the value we obtain is 0.18 K which is nonsensical for a WIM-dominated ISM.

3 DISCUSSION

Long-period pulsars are known to show turnovers in their flux density spectra at frequencies of $\sim 100 \text{ MHz}$ (Maron et al. 2000). It is proposed that at such low frequencies, the radio emission becomes optically thick because of synchrotron self-absorption (O'Dea 1998, Chevalier 1998). From the thermal absorption model, it is seen that if the pulsar were to lie in an extremely dense environment, free-free absorption in the dense region can dominate at frequencies higher than 100 MHz depending on the electron density and electron temperature of the environment. This results in the pulsar flux being absorbed by the surrounding material, which manifests itself as a high-frequency turnover. This study is consistent with the claim that GPS behaviour does not depend on the DM of the pulsar (K11; Dembska et al. 2014). All pulsars lying in a high electron density environment would invariably have high DMs but we measure a higher DM even if the pulsar is further away from us and not necessarily in a dense environment. If this were not true, all pulsars with a high DM would have shown GPS-like characteristics. It is important to note that only pulsars where the line of sight traverses through such dense filaments might show GPS behaviour. We derive large values for the EM for which we consider two physical scenarios based on previous studies (Dulk & Slee, 1975; Lewandowski et al. 2015). Either the pulsar flux is absorbed by the high density, ionized filaments surrounding the PWNs/SNRs or by the cold, partially ionized clouds along the line of sight. Using this idea, and the fact that the absorbers only contribute to a

PSR	α	τ	EM (10^6 pc cm $^{-6}$)		ν_{peak} (GHz)	χ^2 Model	χ^2 Power law
			5000K	30K			
B1054–62	–2.8(8)	0.19(3)	1.1(9)	0.0006(4)	0.6	3.5	6.5
J1809–1917	–2.5(4)	0.16(3)	5.2(3)	0.005(3)	1.8	1.2	7.3
B1822–14	–0.6(1)	0.005(1)	0.2(1)	0.0002(1)	0.7	1.7	16.8
B1823–13	–0.8(1)	0.003(1)	0.5(2)	0.0005(2)	1.0	2.3	46.5
J1740+1000	–2.0(1)	0.007(3)	0.8(1)	0.0008(1)	0.8	12	122.8
J1852–0635	–1.1(1)	0.006(2)	0.7(3)	0.0007(3)	1.0	1.3	3.8

Table 1. For each pulsar, we list the derived values of α and τ from fitting Equation 2 to the spectra. Also listed are the assumed electron temperature and derived EM using Equation 3, ν_{peak} calculated from Equation 4 as well as the reduced χ^2 values from fitting out model versus a simple power law. Figures in parentheses represent the formal uncertainties in the least significant digits.

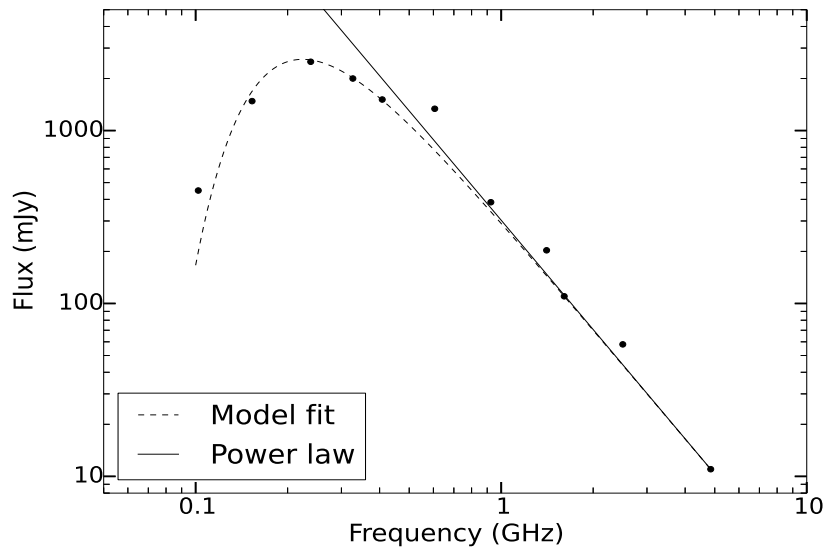


Figure 1. Power law spectrum (solid line) and the best fit curve (dashed line) from the model for PSR B0329+54. The black filled circles are measured flux densities taken from literature. The power law has a spectral index $\alpha = -2.1$ taken from the literature. The model fit has a reduced χ^2 value of 1.8.

PSR	Electron density (cm $^{-3}$)		Linear size (pc)		Absorber
	5000 K	30 K	5000 K	30 K	
B1054–62	3.6×10^3	3.6	0.044	48	Cold, partially ionized cloud
J1809–1917	5.3×10^4	53.5	0.002	1.8	Cold, partially ionized cloud
B1822–14	0.9×10^3	0.9	0.2	195	Dense, ionized filament
B1823–13	4.0×10^3	4.2	0.02	27.2	Dense, ionized filament
J1740+1000	6.6×10^4	66	0.0002	0.2	Cold, partially ionized cloud
J1852–0635	8.0×10^3	7.7	0.01	11	Cold, partially ionized cloud

Table 2. Constrained parameters for all GPS pulsars in our sample by assuming an absorber contribution of 50% to the total DM of the pulsar. To infer the absorber, we assumed $n_e = 100\text{--}6000$ cm $^{-3}$ for a dense, ionized filament and $n_e = 1\text{--}100$ cm $^{-3}$ for a cold, partially ionized cloud and also considered the known environment around the pulsar. PSR B1054–62 was an exception (see text for details).

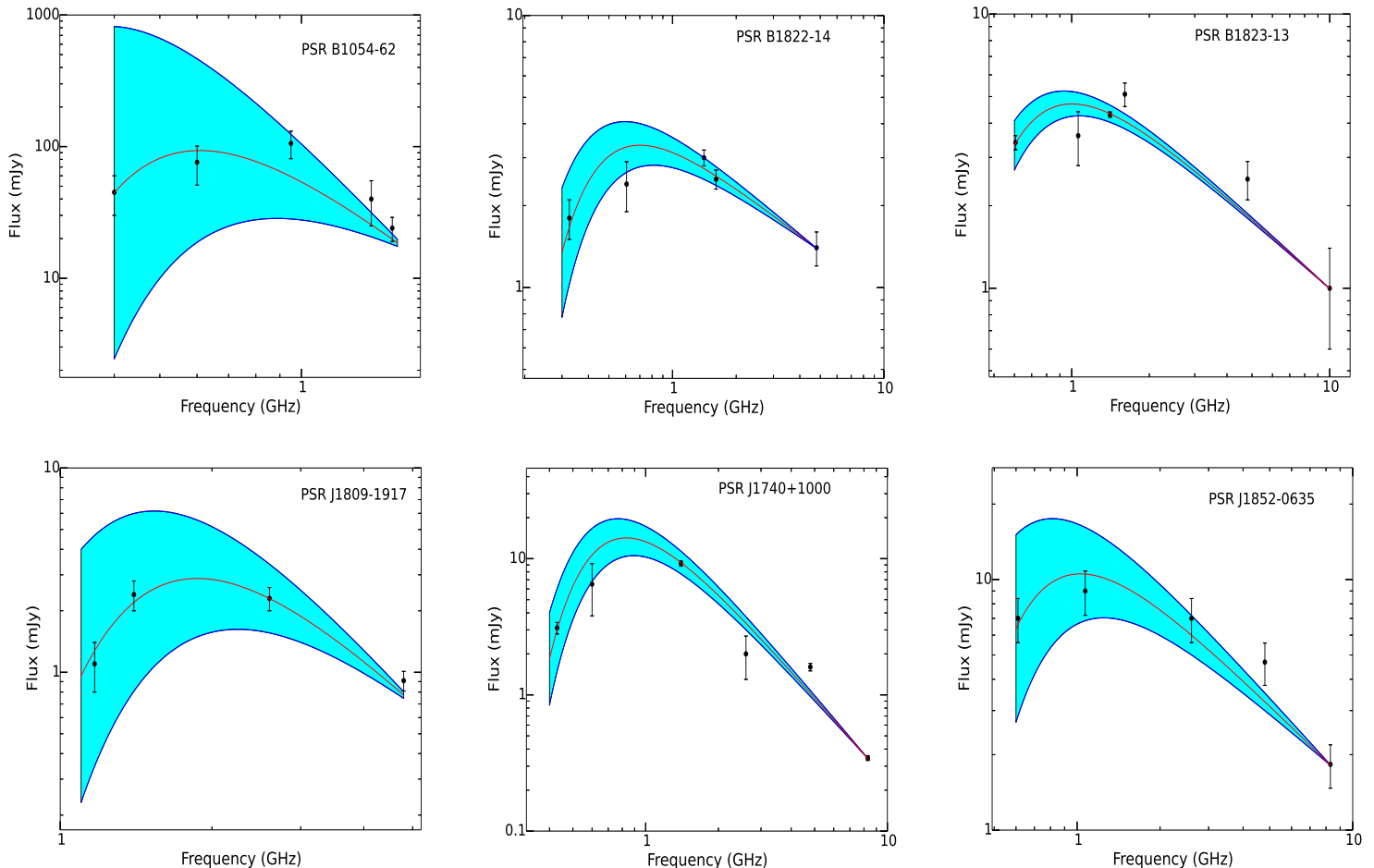


Figure 2. Best fit curve along with $\pm 1\sigma$ region (shaded) obtained from the thermal absorption model for the set of GPS pulsars. Black circles are measured flux densities taken from K07, K11 & Dembska et al. (2014). The $\pm 1\sigma$ shaded region is determined by assuming a Gaussian error on the derived parameters and using $\pm 1\sigma$ limits of these parameters to obtain the curves.

part of the observed DM, we calculate the mean electron density of the absorbers. Assuming a certain range of values of n_e for each scenario ($n_e \sim 100\text{--}6000\text{ cm}^{-3}$ for SNR filaments and $n_e \sim 1\text{--}100\text{ cm}^{-3}$ for cold molecular clouds) and considering the known environment of each pulsar, we report the most plausible absorber for each pulsar in our sample in Table 2. For PSR B1054–62, both the scenarios give reasonable estimates for the electron densities. We believe that a cold absorber is more suitable because, although the pulsar lies near an H II region RCW55 (Koribalski et al. 1995), it lies at the very edge of the region so there is not enough high density, ionized material to produce the observed spectrum. Also, the fact that PSR B1054–62 lies in the Carina complex, a large molecular complex with high star formation, strengthens our claim. The calculations of electron density provides an independent estimate of electron densities within the dense clumps of the ISM that can be very difficult to obtain by conventional methods as most of emission we detect from these sources is non-thermal synchrotron emission (Kargaltsev et al. 2007).

The model also can be useful to gain insights into the emission physics of millisecond pulsars. Investigations in the past have not shown any trend of a turnover in millise-

cond pulsar spectra (Kramer et al. 1999). In recent years, however, with the advent of high sensitivity data acquisition systems, these pulsars are routinely detectable over a wide range of radio frequencies. Recent work by Kuniyoshi et al. 2015 shows that a number of millisecond pulsars are likely to have spectral turnovers at frequencies in the range 0.5–1 GHz. A future application of this model will be to investigate whether any of these pulsars lie within dense environments and use the model to probe the ISM in the vicinity of the pulsar.

The size and characteristics of the pulsar population in the Galactic centre (GC) has been a puzzle for astronomers for the past few years. Several authors have tried to constrain the population of pulsars in the GC using various techniques (see, e.g., Chennamangalam & Lorimer 2014; Macquart & Kanekar 2015) that try to account for a number of observational selection effects. The model discussed here might have potential implications on such work. If we adopt values from the literature for model parameters for a line of sight to the GC, $EM = 5 \times 10^5\text{ cm}^{-6}\text{ pc}$ and $T_e = 5000\text{ K}$ (see, e.g., Pedlar et al. 1989), and take a distribution of intrinsic power-law spectral indices with mean -1.4 and unit standard deviation (Bates et al. 2013), using equation 4,

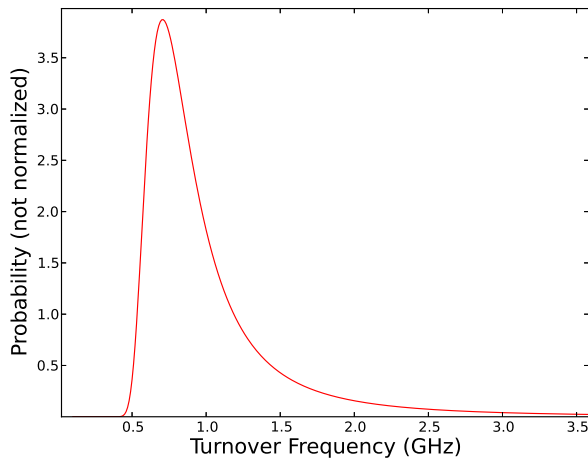


Figure 3. Sample expected probability density function of turnover frequencies for a putative line-of-sight to the Galactic center obtained using Equation 4 and assuming a distribution of spectral indices for a sample population of pulsars in the Galactic center (see text).

it is straightforward to show that there is a distribution of turnover frequencies that extends down to a GHz (see Fig. 3). This distribution suggests that approximately half of all GC pulsars might exhibit spectral turnovers at frequencies greater than 1 GHz. Such pulsars would be harder to detect than previously thought. Recently, there have been targeted pulsar surveys of the GC at frequencies higher than 1 GHz (see, e.g., Macquart et al. 2010; Deneva 2010) that should not be greatly affected by the spectral turnovers. The absence of any detected pulsars in these surveys led Chenamangalam & Lorimer (2014) to conclude that there are very few of these sources in the GC. The results found here suggest that the detectability of pulsars in the GC region may be impacted by spectral turnovers due to the dense environment. We plan to quantify the impacts of this issue on GC pulsar population size constraints further in a future paper.

In summary, we have presented an application of a simple free-free absorption model, also proposed by Lewandowski et al. (2015), which is consistent with the turnover in the spectra of GPS pulsars being caused by propagation through a dense medium. The results of the thermal absorption model strengthen the claim that high-frequency spectral turnovers have their origins in the medium surrounding the neutron star. We were able to determine the most sensible source of absorption for each pulsar using an estimate for the mean electron density within the cloud. More refined measurements of pulsar fluxes, and more examples of GPS pulsars, are essential to test the model further.

ACKNOWLEDGEMENTS

We thank the referee for the comments that greatly improved the paper. This work was supported by a NASA grant (Proposal number: 74279).

REFERENCES

- Altenhoff W. J., Mezger P.G., Wendker H., Westerhout G., 1960, Veröff. Sternwarte, Bonn, No. 59, p.48
- Bates S. D., Lorimer D. R., Verbiest J. P. W., 2013, MNRAS, 431, 2, 1352
- Bates S. D., Lorimer D. R., Rane A., Swiggum J., 2014, MNRAS, 439, 3, 2893
- Berkhuijsen E. M., Muller P., 2008, A&A, 490, 1, 179
- Briskin W. F., Benson J. M., Goss W. M., Thorsett S. E., 2002, ApJ, 571, 906
- Burke, B. F., Graham-Smith, F., 2014, Cambridge University Press
- Chenamangalam J., Lorimer D. R., 2014, MNRAS, 440, 1, L86
- Chevalier R. A., 1998, ApJ, 499, 2, 810
- Churchwell E., 2002, Annual Review of Astronomy and Astrophysics, 40, 27
- Contopoulos I., Spitkovski A., 2006, ApJ, 643, 2, 1139
- Dembka M., Kijak J., Jessner A., Lewandowski W., Bhat-tacharya B., Gupta Y., 2014, MNRAS, 445, 3, 3105
- Deneva I. S., 2010, Ph.D. thesis, Cornell University
- Dulk G. A., Slee O. B., 1975, ApJ, 199, 1, 61
- Graham-Smith, F., 2003, Reports on Progress in Physics, 66, 173
- Kargaltsev O., Pavlov G. G., Garmire G. P., 2007, ApJ, 660, 2, 1413
- Kijak J., Gupta Y., Krzeszowski K., 2007, A&A, 462, 699
- Kijak J., Lewandowski W., Maron O., Gupta Y., Jessner A., 2011, K11, A&A, 531, 16
- Kijak J., Dembska M., Lewandowski W., Melikidze G., Sendyk M., 2011, K11a, MNRAS Letters, 418, 1, 114
- Kijak J., Tarczewski L., Lewandowski W., Melikidze G., 2013, ApJ, 772, 1
- Koo B., Moon D., Lee H., Matthews K., 2007, ApJ, 657, 1
- Koribalski B., Johnston H., Weisberg J. M., Wilson W., 1995, ApJ, 441, 2
- Kramer M., Lange C., Lorimer D. R., Backer D. C., Xilouris K. M., Jessner A., Wielebinski R., 1999, ApJ, 526, 2, 957
- Kramer M., Karastergiou A., Gupta Y., Johnston S., Bhat N. D. R., Lyne A. G., 2003, A&A, 407, 655
- Kuniyoshi M., Verbiest J. P. W., Lee K. J., Adebahr B., Kramer M., Noustos A., 2015, MNRAS, 453, 1, 828
- Lewandowski W., Rozko K., Kijak J., Melikidze G. I., 2015, ApJ, 808, 1, 18
- Lorimer D. R., Yates J. A., Lyne A. G., Gould D. M., 1995, MNRAS, 273, 2, 411
- Macquart J. P., Kanekar N., Frail D. A., Ransom S. M., 2010, ApJ, 715, 2, 939
- Macquart J. P., Kanekar N. 2015, ApJ, 805, 2, 172
- Madsen G. J., Reynolds R. J., Haffner L. M., 2006, ApJ, 652, 1, 401
- Maron O., Kijak J., Kramer M., Wielebinski R., 2000, A&A, 147, 195
- Melrose D. B., Yuen R., 2014, MNRAS, 437, 1, 262
- Mezger P. G., Henderson A. P., 1967, ApJ, 147, 471
- O’Dea C., 1998, PASP, 110, 747, 493
- Pedlar A., Ananthramaiah K., Ekers R.D., Goss W. M., Van Gorkom J. H., Schwarz U. J., Zhao J. H., 1989, ApJ, 342, 769
- Press W. H., Flannery B. P., Teukolsky S. A., Vetterling W. T., Numerical Recipes in C, 2010, Cambridge University

Press

Sankrit R., Hester J., Scowen P. A., Ballester G. E., Burrows C. J., Clarke J. T., Crisp D., Evans R. W., Gallagher J. S. III., Griffiths R. E., Hoessel J. G., Holtzman J. A., Krist J., Mould J. R., Stapelfeldt K. R., Trauger J. T., Watson A., Westphal J. A., 1998, *ApJ*, 504, 1
Sieber W., 1973, *A&A*, 28, 237
Slane P., Helfand D. J., Van Der Swaluw E., Murray S. S., 2004, *ApJ*, 616, 1, 403